Available online at www.CivileJournal.org

Civil Engineering Journal

(E-ISSN: 2476-3055; ISSN: 2676-6957)

Vol. 10, No. 02, February, 2024

Experimental and Numerical Analysis of Concrete Columns under Axial Load Based on European Design Norms

Florim Grajçevci [1], Armend Mujaj [1*], Driton Kryeziu [2], Elfrida Shehu [3]

[1] *Faculty of Civil Engineering, University of Pristina, Pristina, Kosovo.*

[2] *Civil Engineering and Infrastructure Department, University for Business and Technology UBT, Pristina, Kosovo.*

[3] *Polytechnic University of Tirana, Tirana, Albania.*

Received 16 October 2023; Revised 17 January 2024; Accepted 21 January 2024; Published 01 February 2024

Abstract

This study presents a comparison between numerical and experimental results for reinforced concrete columns subjected to axial compression. Depending on the columns support and their organization within the structure, columns primarily work under either concentric or eccentric compression, respectively, bending in situations where horizontal actions such as wind or/and earthquakes are present in the structure. Different countries have specific design codes, and in this study, the calculation of columns is based on the European design codes, specifically EN 1992-1-1. As a common practice in most cases during research, tests are conducted using computational models, and based on the obtained results through the application of similarity theory, an attempt is made to transition to the actual behavior of structural elements. Therefore, this paper applies a logic of "almost real" testing, where two columns with square cross-sections were produced and tested. The columns had a rectangular base with cross-section dimensions of 20/20 cm and a height (L) of 300 cm, with a concrete strength of $f_{cm,cube}$=61.80 MPa. They were reinforced with longitudinal reinforcement (4Ø12 mm) and had a tensile strength of f_{tm}=588.10 MPa. Additionally, stirrups of Ø8 mm were placed at every s_w=25 cm. Experimental results show a closer alignment with software calculations using SEISMOSOFT with an accuracy of 96%, while results according to EN 1992-1-1, based on simplified methods, show 64% for the Nominal Stiffness Method and 59% for the Curvature Method.

Keywords: Concrete Structures; Column Capacity; Experiment; Strain-Gage; Lateral Displacement.

1. Introduction

Reinforced concrete structures are among the most applied and popular structures in the field of civil engineering worldwide. Consequently, numerous theoretical and experimental studies have been conducted by various researchers and institutions. Scientific findings from these studies have led to the development of design codes, one of which is EN 1992-1-1 [1], applied in European Union countries. Over time, design codes undergo modifications and additions, especially after natural phenomena, by revising existing parameters and replacing them with new ones. Every structural member holds its own significance, and among them, columns require special attention. Columns primarily undergo axial forces in compression, but depending on the boundary conditions and nature of actions, they also experience bending, shear, and interaction between them [2]. Reinforced concrete members play a crucial role in resisting the collapse of superstructures, necessitating further investigation into their fatigue performance. Columns must be designed in a way that ensures sufficient stability, aiming to achieve the intended sustainability of the structures [3].

* Corresponding author: armend.mujaj@uni-pr.edu

http://dx.doi.org/10.28991/CEJ-2024-010-02-05

During the calculations of these structural elements, local and global stability conditions must be controlled, including the effects of imperfections, the second-order theory for highly bent columns (long columns), the sway effect (lack of straightness), mechanical nonlinearity of the material, and the effects arising from deformations, such as shrinkage and creep [1, 4-6]. In the theoretical treatment of columns within this work, both linear analyses, considering simplified calculation methods, and nonlinear analysis, involving software calculations, have been taken into account [1, 7, 8]. Under axial compression loading, especially in cases with eccentricity (bending moments at the edges), vertical structural members or columns experience additional bending. This phenomenon leads to an increase in the initial bending moment (first-order theory) known as the $P - \Delta$ effect, which is crucial to be checked, particularly in the case of slender and curved columns where it often proves to be significant during the calculation phase [9]. The geometric ratio of their dimensions is also important alongside the material properties for the load-bearing capacity (collapse) of columns. This ratio involves the relationship between the height and the cross-sectional dimension of the columns, where the mechanism of failure depends on this ratio.

If the ratio of L/b is less than 20, the failure of the column is expected to occur as a consequence of concrete failure. On the other hand, if the ratio L/b is greater than 20, the collapse of the column is expected to happen due to the loss of global stability, expressing the critical force [10]. Dundar et al. [11] conducted experimental treatments on elements subjected to biaxial compression, testing columns with various cross-sectional dimensions. Their main goal was to analyze the effect of load eccentricity. Besides the dimensions of the cross-section, material properties, static schemes, and the longitudinal reinforcement area, the area of transverse reinforcement (stirrups) also has a significant effect on the load-bearing capacity of columns [12, 13]. During the design of reinforced concrete members, the approach to problem-solving is crucial, especially the selection of calculation methods. A study on the simplified design procedures for reinforced concrete columns based on the concept of the equivalent column was carried out by authors such as Afefy et al. [14]. Despite numerous theoretical and experimental studies on the addressed issue by various researchers, there are few comparisons between experimental results and those provided by calculation methods included in the framework of EN 1992-1-1 [1]. This was the main objective of the work.

The significance of this study was to present the behavior of reinforced concrete columns under the influence of axial compressive force, specifically focusing on the case of symmetric eccentricity. The study involved analysing and comparing experimentally obtained values with theoretical ones according to EN 1992-1-1, as well as results from the SEISMOSOFT software applications. The interpretation of the output results included parameters such as maximum force, lateral displacement at the mid-span of the columns, axial displacement, as well as values of deformations and stresses in the concrete.

2. Experimental Program

2.1. General Description

In this study, two columns possessing identical characteristics and parameters were created and examined for both material properties and geometry, employing the same static scheme, as presented in Figure 1 and Table 1. This approach was adopted to enhance the reliability and comparability of the obtained results.

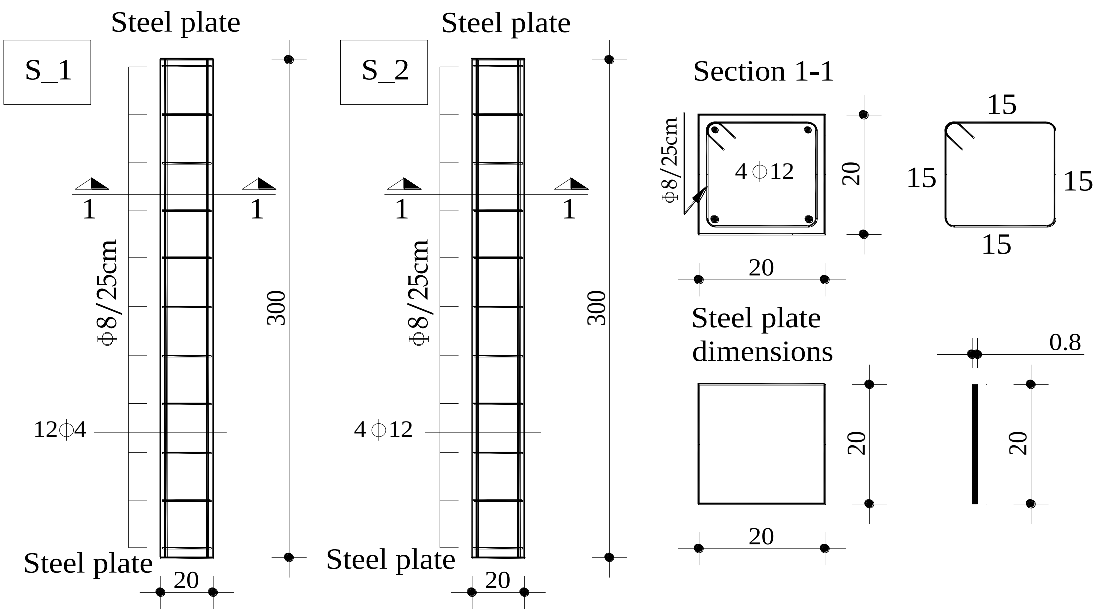

Figure 1. Details of test specimens (unit: cm)

Table 1. The Geometric Characteristics of Column Samples

Sample No.	Dimension b (mm)	Dimension h (mm)	Length (mm)	e_A (mm)	e_B (mm)	As (mm^2)	Sw (mm)
S-1	200	200	3000	30	30	452	250
S-2	200	200	3000	30	30	452	250

For the computation of the theoretical problem, Figure 2 is shown the block diagram explaining the steps of the analysis respecting the standard of EN 1992-1-1 [1] and Bond et al [15].

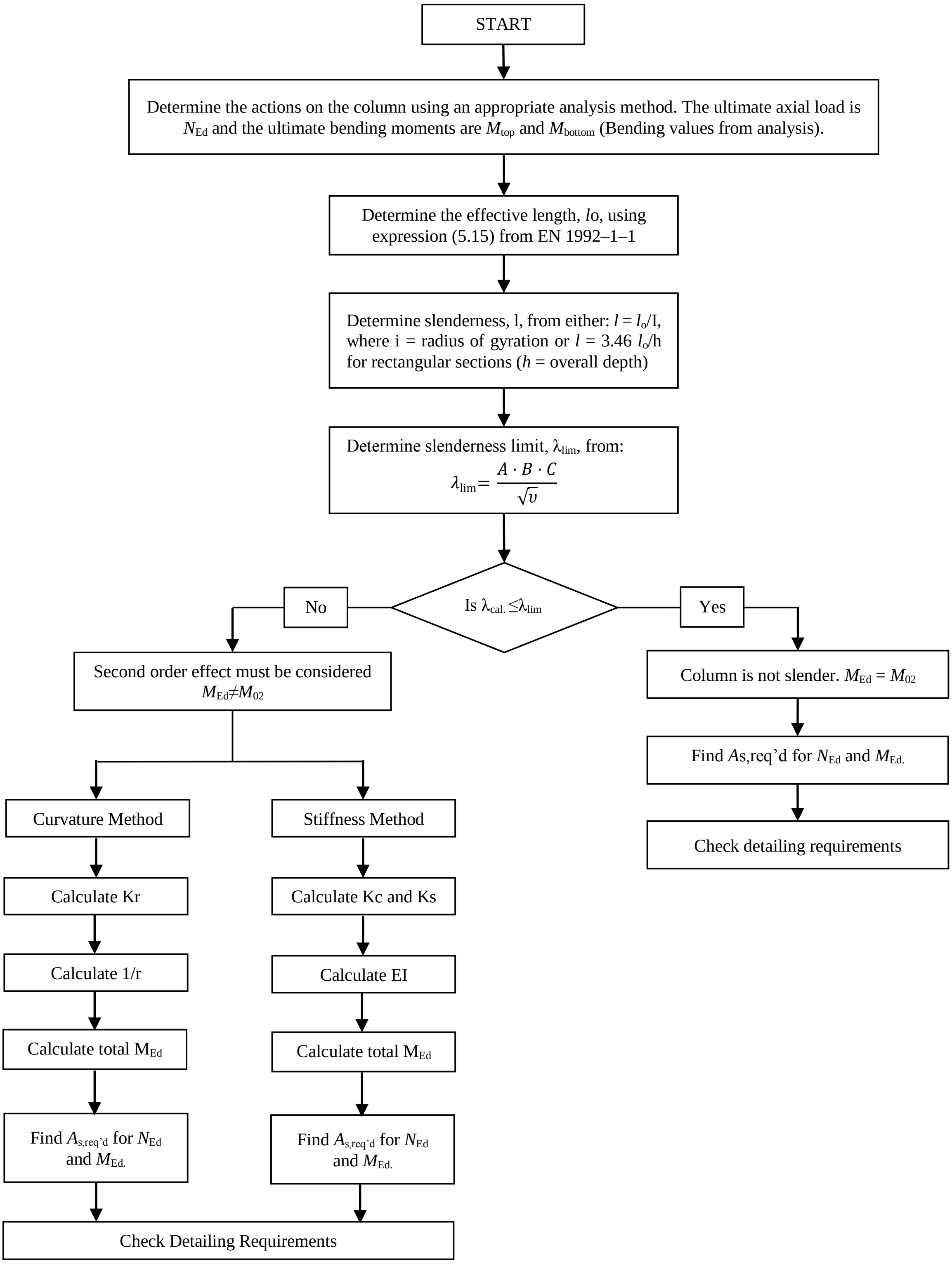

Figure 2. Flow chart for column design

The procedures involved in crafting experimental samples include the formulation and preparation of concrete mixtures, the assembly of the reinforcement structure (both longitudinal and stirrups), the preparation and securing of moulds, and ultimately, the pouring of concrete (Figure 3). The details of the concrete mixture are shown in Tables 2 and 3. To optimally apply axial force in the members, support heads are fashioned as hinges using steel plates, ensuring a uniform load distribution across the cross-sections. To mitigate local stress on the initial cross-section, 3 mm-thick steel plates are welded onto the longitudinal reinforcement.

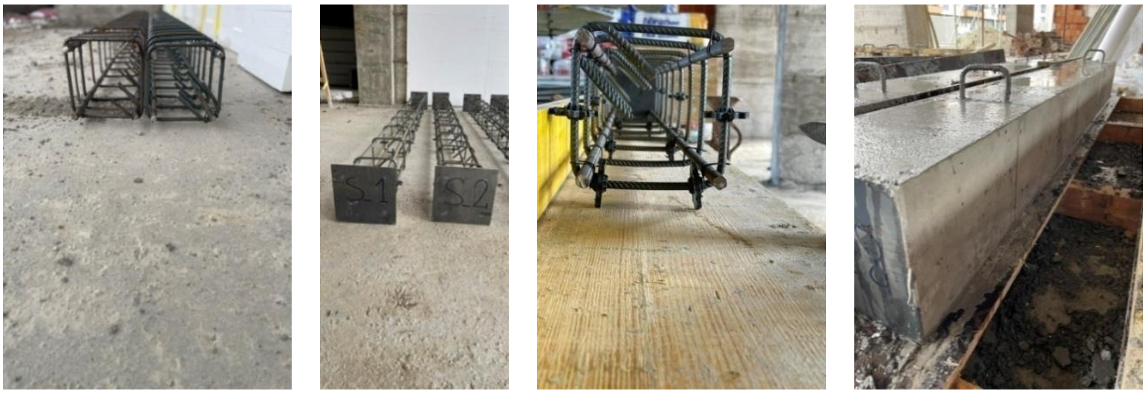

(a) (b) (c) (d)

Figure 3. Stage of sample preparation (a) reinforcement, (b) steel plates welded into the reinforcement, (c) concrete cover, (d) casting concrete

Table 2. Concrete mixture proportions

Concrete Mix-Design	Cement CEM II/B-M(W-L) 42.5 R (kg/m^3)	Total water content (kg/m^3)	Effective w_{eff}/c ratio	Super plasticizer HiperPlast 235 LT (%)	Natural aggregate (NA), (kg/m^3)		
					0/4	4/8	8/16
	380	177	0.45	0.60	1048	353	460

Table 3. Mechanical properties of the reinforcement

Sample No.	Diameter (mm)	Length (mm)	Area (mm^2)	Mass (kg)	Tensile Strength (Rm) (MPa)	Yield Strength (ReH) (MPa)	Ductility $(k=ft/fy)_k$	Elasticity Modulus E (MPa)	Percentage elongation A (%)
M-1	8.06	558	51.00	0.22	599.6	514.9	1.164	189254	9.22
	8.00	558	50.20	0.22	601.7	527.1	1.142	200463	16.32
	8.07	557	51.10	0.22	604.2	532.5	1.134	173473	14.42
M-2	12.00	549	112.9	0.49	680.2	586.5	1.160	195421	12.62
	9.99	549	112.8	0.49	693.2	597.3	1.161	176448	12.05
	11.97	553	112.5	0.49	679.5	582.4	1.165	183623	11.72

To establish an ideal boundary condition [16] for the samples, steel jaws equipped with connectors, essential bolts, and steel plates are fabricated, as shown in the Figure 4.

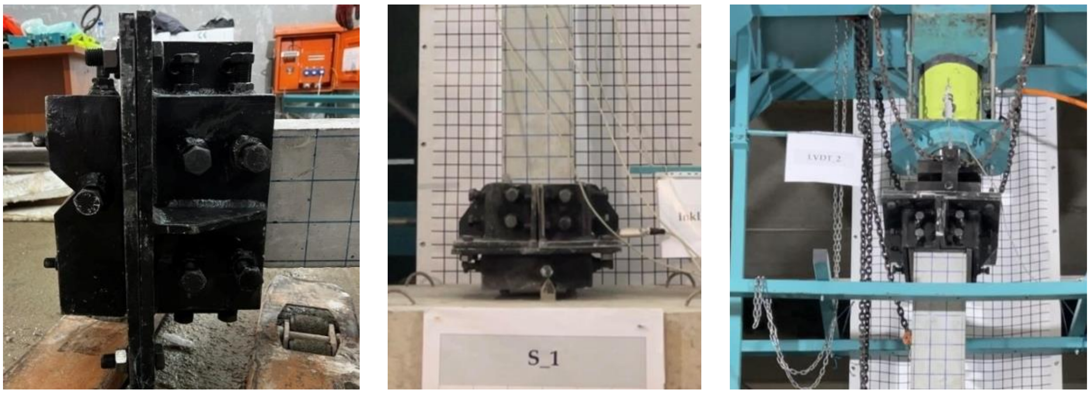

(a) (b) (c)

Figure 4. (a) Model of the steel jaws connectors, (b) samples connector – boundary condition – bottom support, (c) samples connector boundary support on top

From the longitudinal reinforcements are taken the experimental samples for the examination of mechanical properties, which were made in the accredited laboratories "ACT -ing "located in the City of Pristina, as is shown in Figure 5.

(a) (b) (c)

Figure 5. Mechanical property of reinforcement tests (a) taken samples, (b) samples during the test in tensile, (c) moment of reinforcement failure

In the table below are shown the mechanical results from the reinforced samples based on standards EN ISO 15630-1 [17]. Also, during the concreting of the columns, cubic specimens were taken to evaluate the mechanical properties of the concrete, which were maintained and tested in the accredited laboratory "ACT-ing" based in Pristina, as presented in the following part of the work (Figure 6).

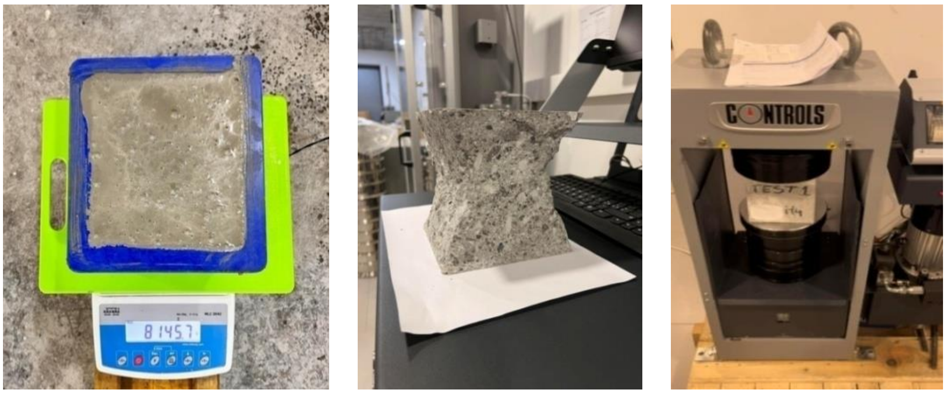

(a) (b) (c)

Figure 6. Concrete units' preparation for the mechanical examination (a) Taken units, (b) Unit during the examination, (c) After unit examination

After making and curing the concrete specimens in laboratory conditions according to EN 12390-2 [18]. Standard and based on EN 12390-3 [19]. Standard after 2, 3, 7 and 28 days, the specimens were tested and the output results were obtained as presented in Table 4.

Table 2. Mechanical properties and strengthening of the concrete units taken from the columns

Sample No.	Apparent density (kg/m^3)	Age (days)	Maximum load (kN)	Cross-sectional area (mm^2)	Compressive strength (MPa)
M-1	2420	2	587.1	22500	26.10
M-2	2420	2	608.1	22500	27.00
Average	**2420**		**597.6**		**26.60**
M-3	2420	3	752.0	22500	33.40
M-4	2450	3	766.5	22500	34.10
Average	**2430**		**759.3**		**33.70**
M-5	2430	7	977.1	22500	43.40
M-6	2410	7	1044.5	22500	46.40
Average	**2420**		**1010.8**		**44.90**
M-7	2440	28	1410.3	22500	62.70
M-8	2440	28	1307.6	22500	58.10
M-9	2440	28	1425.2	22500	63.30
M-10	2440	28	1441.2	22500	64.10
M-11	2440	28	1343.2	22500	59.70
M-12	2450	28	1409.3	22500	62.60
Average	**2430**				**61.80**

The achieved real results from the examination of the reinforcing units and the concrete units are used in the software for the theoretical analysis of the axial compression of columns. The representative value of the compressive strength of the concrete was $f_{cm,cube}$=61.80 MPa and for the reinforcing bar was f_{tm}=588.10MPa.

For precise and reliable examination, results were requested from the laboratory of "ProIng", Pristina, in order to calibrate the exanimating machine–piston, as shown in Figure 7. The calibration of the hydraulic piston has been made via the equipment of "HBM Quantum X" and validated force of pressure was within accuracy of +/-0.50 kN.

Figure 7. The piston calibration

In the erected column samples, the necessary measuring equipment is installed on the steel frame. This is for obtaining proper, precise, and reliable final results regarding the behavior. Equipment such as the "load cell" is used for monitoring the applied load, LVDT for measuring the horizontal and vertical displacement of the samples, monitoring the inclined deformation through an inclinometer, and four strain gauges are installed for measuring the deformation, as shown in the figure below (Figure 8) [20, 21].

(a) (b) (c) (d)

Figure 8. Sample erected for testing (a) columns' marking, (b) Strain gauges installation, (c) LVDT and SG, (d) Inclinometer

The slenderness ratio influences the mode of failure of the element. If the ratio l_e/i is less than 50, then the column is expected to fail in concrete due to crushing, and the failure is not caused by bending. However, when the slenderness ratio l_e/i is greater than 110, the failure will occur due to buckling as a result of bending. In the case of this study, the slenderness ratio is close to the value of 51.90, which is near 50. As observed in the figures below (Figure 9), the failure of the column was caused by concrete crushing rather than bending [6].

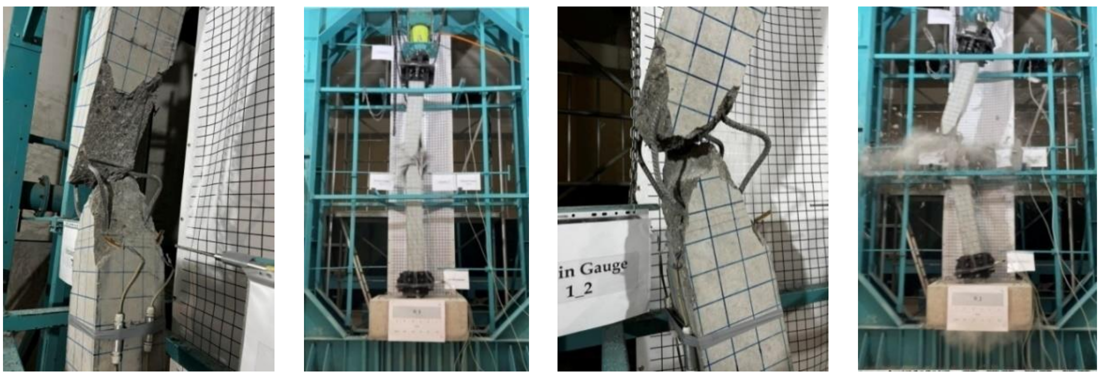

(a) (b) (c) (d)

Figure 9. Sample after the testing (a) Local collapse of the concrete, (b) Moment of collapse, (c) collapse of the reinforcement, (d) in front of collapsing

The anticipated failure of the samples has two possible scenarios. One is the potential collapse of the concrete cross-section due to local instability caused by the ratio of the column length to the dimension of the cross-section, i.e., 3000/200=15<20. The other scenario is the overall loss of stability as a consequence of slenderness, which is not applicable in our case [10].

During the monitoring of the column's behavior and the assessment of result reliability, equipment calibration, pre-installation testing of equipment, and the installation of sensitive strain gauges (SG), the applied load on the samples is quasi static and shall be increased in increments, as illustrated in the Figure 10 [22, 23].

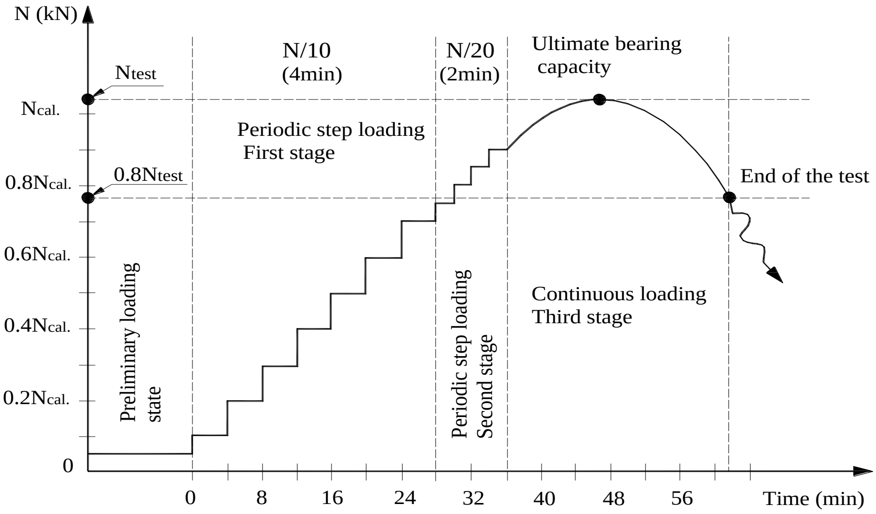

Figure 10. Incremental load applying diagram

All measurements during the examinations are captured digitally via LVDT and Strain Gauge on the "HBM Quantum X" equipment and transformed into numerical and graphical data by the computer (see Figure 11 to 13) [23, 24].

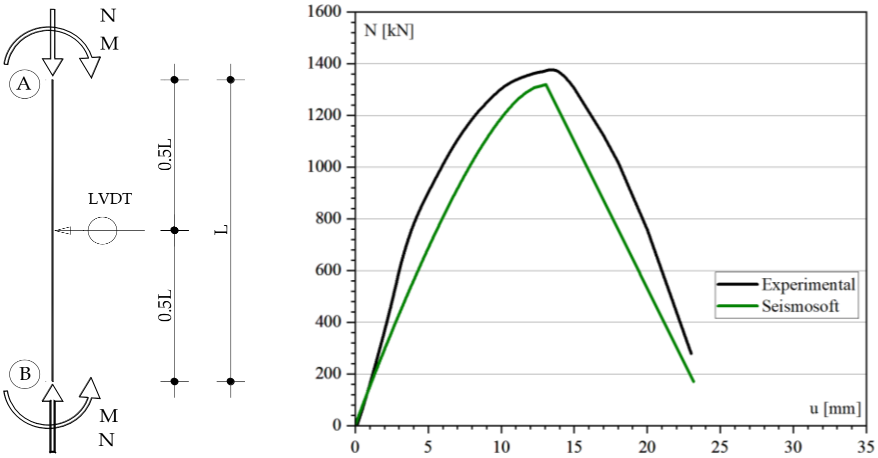

Figure 11. Graphical presentation of the diagram force–lateral displacements

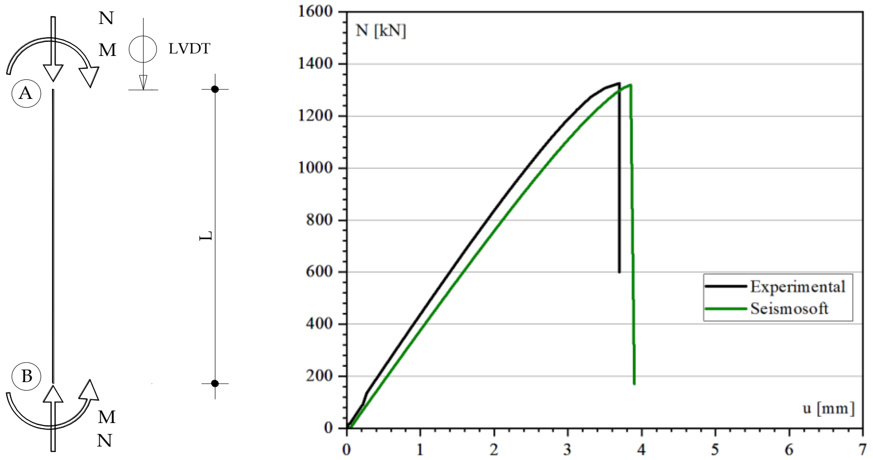

Figure 12. Graphical presentation of the diagram force-axial displacement

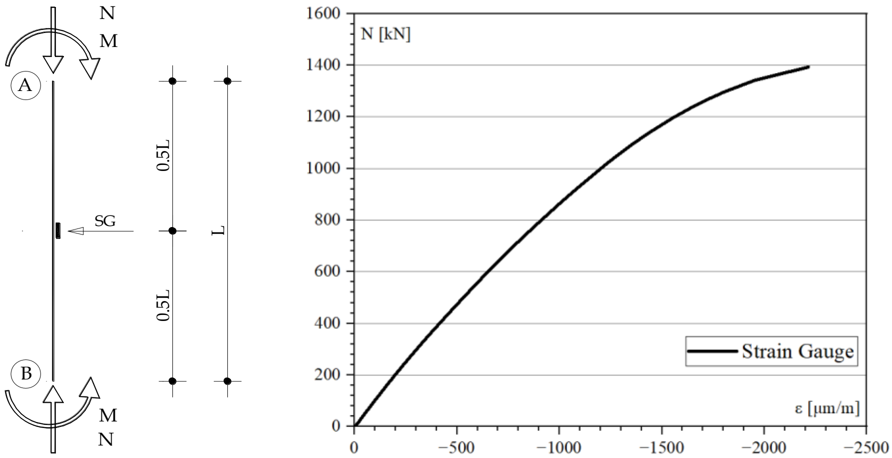

Figure 13. Graphical presentation of the diagram force- -deformation

The concrete compressive strength value of $f_{cm,cube}$=61.80 MPa, in accordance with the EN 206 [26] response the concrete class of C45/55 were the young modulus has the value of E_{cm}=360,000 MPa according to EN 1992-1-1 [1]. Based on principle of Hooke's Law, the strained state of cross section – compression zone, in the middle length of the column has been calculated as $\sigma=\varepsilon \cdot E_{cm}=2150 \cdot 36000 \cdot 10^{-6}=77.40$ MPa.

3. Theoretical Approach

The nonlinear computation of the structural member is thoroughly considered to obtain reliable results regarding the behavior of the scrutinized material. The second theory, referring to columns, usually involves calculations with greater steps, and the use of professional software saves time for problem-solving. However, for a more practical computation, different methods allowed in the code, known as methods of stiffness and/or curvature, are employed [1, 26].

For the single column, the value of bending moment included part from the second theory has:

$$\mathrm{M_{Ed}} = \mathrm{M_{0Ed}} + \mathrm{M_2} = \mathrm{M_{0Ed}} + \mathrm{N_{Ed}} \cdot \mathrm{y} = \mathrm{M_{0Ed}} + \mathrm{N_{Ed}} \cdot \frac{1}{\mathrm{r}} \cdot \frac{\mathrm{l}^2}{\mathrm{c}} \tag{1}$$

where M_{Ed} is total bending moment, M_{0Ed} is the first order moment, M_2 is second theory part of bending moment, N_{Ed} is axial compressive force, y is displacement of column in the middle of the spam, $1/r$ is ratio of the curvature, l is length of the column, c is factor for coefficient curvature distribution.

In the Stiffness Method use, the ratio of curvature is:

$$\frac{1}{r} = \frac{M_{Ed}}{EI} \tag{2}$$

The nominal stiffness has the equation of:

$$\mathrm{EI}=\mathrm{K}_c E_{\mathrm{cd}} I_c+\mathrm{K}_s E_s I_s \tag{3}$$

In the ratio of the percentage of cross-section reinforcement:

$$\rho=\frac{A_{\mathrm{sl}}}{A_c} \geq 0.002 \tag{4}$$

where $\mathrm{K_s}$= 1- reinforced contribution factor, $\mathrm{K_c} = \frac{\mathrm{k_1 \cdot k_2}}{1+\varphi_{\mathrm{ef}}}$; depends on concrete rheology:

$$k_1 = \sqrt{\frac{f_{\mathrm{ck}}}{20}} \tag{5}$$

$$\mathrm{k_2} = \nu \cdot \frac{\lambda}{170} \leq 0.20 \tag{6}$$

$$\nu = \frac{\mathrm{N_{Ed}}}{\mathrm{A_c \cdot f_{cd}}} \tag{7}$$

$$\mathrm{K_c} = \frac{\mathrm{k_1 \cdot k_2}}{1+\varphi_{\mathrm{ef}}} \tag{8}$$

$$\rho=\frac{A_{\mathrm{sl}}}{A_c} \geq 0.001 \tag{9}$$

where $\mathrm{K_s}$=0-reinforced contribution factor, $\mathrm{K_c} = \frac{0.3}{(1+0.5\varphi_{\mathrm{ef}})}$, depends on concrete rheology, $\mathrm{E_{cd}} = \frac{\mathrm{E_{cm}}}{\gamma_{\mathrm{CE}}}$, $\mathrm{E_s}=20000\mathrm{kN/cm^2}$.

where ρ -is the geometrical reinforcement ratio, As/Ac, φ_{ef} is the effective creep ratio, k_1 is depends on concrete strength class, k_2 is depends on axial force and slenderness, ν is the relative axial force, $N_{Ed}/(A_c f_{cd})$, Ac is the area of concrete cross section, E_c, E_s are concrete and steel moduls of elasticity.

$$M_2 = N_{Ed} \cdot \frac{1}{r} \cdot \frac{l^2}{c} = N_{Ed} \cdot \frac{M_{Ed}}{EI} \cdot \frac{l_o^2}{c} = N_{Ed} \cdot \frac{l_o^2}{EI}\left(\frac{M_{Ed}}{c_o} + \frac{M_2}{c_2}\right) \tag{10}$$

$$M_2 = M_{0Ed} \frac{N_{Ed} \cdot \frac{l_o^2}{c_o \cdot EI}}{1 - N_{Ed} \cdot \frac{l_o^2}{c_2 \cdot EI}} = M_{0Ed} \frac{\frac{c_2}{c_o}}{\frac{c_2 \cdot EI}{N_{Ed} \cdot l_o^2} - 1} \tag{11}$$

The value of c_o coefficient depends on the distribution of static diagrams and the value of $c_2=\pi^2$:

$$M_2 = M_{0Ed} \frac{\frac{\pi^2}{c_o}}{\frac{\pi^2 \cdot EI}{N_{Ed} \cdot l_o^2} - 1} = M_{0Ed} \frac{\beta}{\frac{N_B}{N_{Ed}} - 1} = M_{0Ed}\left(1 + \frac{\beta}{\frac{N_B}{N_{Ed}} - 1}\right) \tag{12}$$

$$N_B = \frac{\pi^2 \cdot EI}{l_o^2} \tag{13}$$

$$\beta = \frac{\pi^2}{c_0} \tag{14}$$

where N_B- is the buckling load based on nominal stiffness, β is parameter taking into account the distribution of first order moment.

As per Curvature Method the interference computation of the vertical elements is:

$$\theta_i = \theta_o \cdot \alpha_h \cdot \alpha_m \tag{15}$$

$$\theta_o = \frac{1}{200}; \alpha_h = \frac{2}{\sqrt{l}}; \alpha_m = \sqrt{\frac{1}{2} \cdot \left(1 + \frac{1}{m}\right)} \tag{16}$$

$$e_a = \theta_i \cdot \frac{l_o}{2} \tag{17}$$

The computation of the eccentricity as per second theory is:

$$e_2 = \frac{1}{r} \cdot \frac{l_o^2}{c} \tag{18}$$

Based on the Curvature Method the curvature computation is different from the previous first presented method:

$$\frac{1}{r} = K_r \cdot K_\varphi \cdot \frac{1}{r_o} = K_r \cdot K_\varphi \cdot \frac{\varepsilon_{yd}}{0.45 \cdot d} = K_r \cdot K_\varphi \cdot \frac{f_{yd}}{0.45 \cdot d \cdot E_s} \tag{19}$$

$$K_r = \frac{(n_u - n)}{(n_u - n_{bal.})} \leq 1{,}0 \tag{20}$$

$$\nu = n = \frac{N_{Ed}}{A_c \cdot f_{cd}}; n_u = 1 + \omega; n_{bal.} = 0.40 \tag{21}$$

$$K_\varphi = 1 + \beta \cdot \varphi_{ef} > 1.0 \tag{22}$$

$$\beta = 0.35 + \frac{f_{cd}}{200} - \frac{\lambda}{150} \tag{23}$$

where θ_i is the general angle, θ_0 is the basic value, α_h is the reduction factor for height or length, α_m is the reduction factor for number of members, l is height or length, m is the number of vertical members contributing to the total effect, K_r is a correction factor depending on axial loads, K_φ is a factor for taking account of creep, λ is the slenderness ratio, θ_i is the general angle, θ_0 is the basic value, α_h is the reduction factor for height or length, α_m is the reduction factor for number of members, l is height or length, m is the number of vertical members contributing to the total effect, K_r is a correction factor depending on axial loads, K_φ is a factor for taking account of creep, λ is the slenderness ratio.

$$N_{Rd} = A_{c,neto} \cdot f_{ck} + A_{sl} \cdot f_{yk} = (b \cdot h - A_{sl}) \cdot f_{ck} + A_{sl} \cdot f_{yk} \tag{24}$$

Based on the used literature the capacity resistance of the columns for the axial loads:

As per theory of the Structure, the displacement from the eccentricity of the compressed members is expressed with equation:

$$w_{l/2} = \frac{3l^2}{48EI} = (M_A + M_B) \cdot \delta \tag{25}$$

The effect of the axial compressive force on the displacement in the middle of the members is:

$$\delta = (\frac{1}{1-\frac{N}{N_B}}) \tag{26}$$

where N is axial action, N_B is Euler critical force, M_A is on top of member bending moment, M_B is on bottom of member bending moment, δ is effect of axial force on the column displacement.

The values of the axial forces and displacements from the experimental and theoretical values given by different computation methods and their ratios are shown in Table 5. The value and ratio of the axial force experimental force and the theoretical values of the force given by different computation methods are presented in Table 6.

Table 3. Values of the axial forces and displacements from the experimental and the theoretical values given by different computation methods and their ratio

Method	N (kN)	w (mm)	$N/N_{exp.}$	$w/w_{exp.}$
Experimental	1379	13.28	1.00	1.00
SEISMOSOFT	1319	13.06	0.96	0.98
Nominal stiffness method	910	50.80	0.66	0.26
Curvature method	815	39.50	0.59	0.34

Table 4. Value and ratio of the axial forces experimental force and the theoretical values of the force given by different computation methods

Method	N (kN)	N_{Rd} (kN)	$N/N_{exp.}$
Experimental	1379	2718	0.50
SEISMOSOFT	1319		0.48
Nominal stiffness method	910		0.34
Curvature method	815		0.30

Having into consideration the load eccentricity effect, using the software SEISMOSOFT the obtained results of axial bearing capacity of columns in variation of the eccentricity are shown in the Table 7.

Table 5. Eccentricity effect on the bearing capacity of columns

Eccentricity $e_A=e_B$ (mm)	30	40	50	60	70	80	90	100
N(kN)	1319	1079	867	703	588	497	423	364
w (mm)	13.06	15.39	18.75	23.26	27.45	29.32	32.66	32.47

Figure 14 is shown the curvature's shape between the axial load and eccentricity applied where in the beginning is linear then by increasing the eccentricity shows to be parabolic.

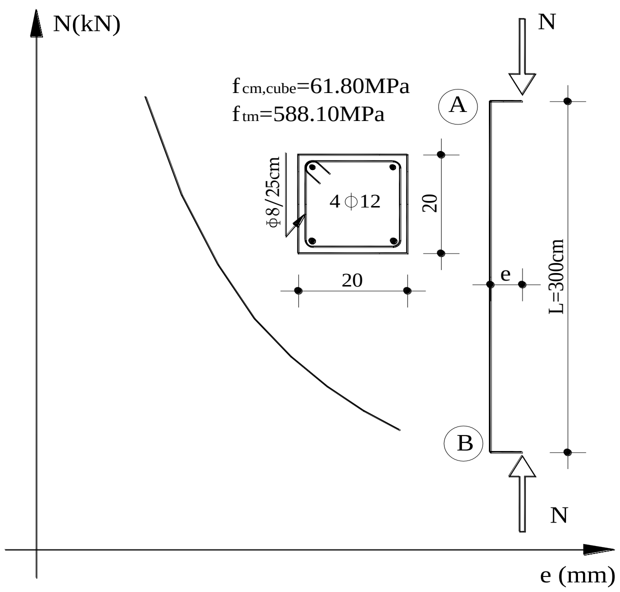

Figure 14. Load – eccentricity curvature

4. Conclusions

The bearing capacity of sensitive vertical structural members is influenced by variations in load and eccentricity. The paper conducts a comparison between theoretical-analytical results and experimental cases of columns, adhering to the standards of EN 1992-1-1. This involves referencing all methods of computation, as well as the simplified methods used in the analysis. The experimental results of mechanical performances for vertical structural members loaded in compression, as evaluated by simplified methods from the Eurocodes, indicate lower accuracy compared to the results obtained from the SEISMOSFT software. The SEISMOSFT software demonstrated 96% accuracy when compared to the results derived from the experimental cases.

As per the Eurocode standards, the characteristic values of the material properties and the actions on the structures are representative, and to be used the design values, the partial safety factor must be taken into consideration. The mentioned partial safety factors naturally account for various effects of the action situations, ULS and SLS for structure, quality variation of concrete, variation of reinforcement, etc. However, in our research, the partial safety factors for the used material and the applied action are not considered for result reliability.

To validate the results obtained from the theoretical description of the second theory for axial compression structural members, further research is recommended. This research should be based on numerous experiments to achieve a proper solution for the collapse of members due to the ratio of $L/b > 20$ or $l_e/i > 50$. Considering that for this paper only two samples were examined, i.e., the small samples may impact the accuracy and representativeness of the results. For more precise and representative findings, it is recommended to increase the number of samples. These additional samples should encompass various material properties, geometric conditions, different loads (quasi-static), and diverse scenarios of load eccentricity.

The obtained test results indicate that the concrete's actual compressive stress in the middle of the column is higher than the actual compressive strength of concrete obtained from the examined cubic specimens, and the difference is 20%. This difference in stresses results from the contribution of longitudinal reinforcement, especially the confinement effect of concrete by stirrups (transverse reinforcement). This phenomenon will be the subject of further research. The effect of the yield and the creep of the concrete is not included in this study, and for future research, including these effects may be in the interest of the given realizable results. Also, for future research, it will be very important to also include the stiffness of the member, respectively, effective stiffness.

5. Declarations

5.1. Author Contributions

Conceptualization, F.G., A.M., D.K., and E.S.; methodology, F.G., A.M., and D.K.; software, F.G., A.M., and D.K.; validation, F.G., A.M., and D.K.; formal analysis, F.G., A.M., D.K., and E.S.; investigation, F.G., A.M., D.K., and E.S.; resources, F.G., A.M., and D.K.; data curation, F.G., A.M, and D.K.; writing—original draft preparation, F.G., A.M., D.K. and E.S.; writing—review and editing, F.G., A.M., D.K., and E.S.; visualization, F.G. and A.M.; supervision, F.G. and E.S.; project administration, F.G., A.M., and D.K.; funding acquisition, F.G., A.M., D.K., and E.S. All authors have read and agreed to the published version of the manuscript.

5.2. Data Availability Statement

The data presented in this study are available in the article.

5.3. Funding

The authors received no financial support for the research, authorship, and/or publication of this article.

5.4. Conflicts of Interest

The authors declare no conflict of interest.

6. References

[1] EN 1992-1-1. (2004). Eurocode 2: Design of concrete Structures-Part 1-1: General rules and rules for buildings. European Committee for Standardization, Brussels, Belgium.

[2] Ahmed, A., Mohammed, A. M. Y., & Maekawa, K. (2021). Performance Comparison of High Strength Reinforced Concrete Circular and Square Columns Subjected to Flexural Controlled Cyclic Loading. Civil Engineering Journal, 7(1), 83–97. doi:10.28991/cej-2021-03091639.

[3] EN 1990. (2002). Eurocode-Basis of structural design. European Committee for Standardization, Brussels, Belgium.

[4] Li, X., Wang, X., Liu, J., & Chen, Y. F. (2023). Behavior and design of eccentrically-loaded slender tubed steel-reinforced high-strength concrete columns. Journal of Constructional Steel Research, 205, 107907. doi:10.1016/j.jcsr.2023.107907.

[5] Westerberg, B. (2008). Time-dependent effects in the analysis and design of slender concrete compression members. Ph.D. Thesis, KTH Royal Institute of Technology, Stockholm, Sweden.

[6] Mosley, W. H., Bungey, J. H., & Hulse, R. (1999). Reinforced Concrete Design. Macmillan Education, London, United Kingdom. doi:10.1007/978-1-349-14911-7.

[7] Amirkhani, S., & Lezgy-Nazargah, M. (2022). Nonlinear finite element analysis of reinforced concrete columns: Evaluation of different modeling approaches for considering stirrup confinement effects. Structural Concrete, 23(5), 2820–2836. doi:10.1002/suco.202100532.

[8] SeismoStruct (2024). Seismosoft. Eshop Designed & Developed by Pontemedia, Pavia, Italy. Available online: https://seismosoft.com/ (accessed on January 2024).

[9] Burgos, R. B., & Silva, L. E. (2023). Evaluation of the P-Δ (P-Delta) effect in columns and frames using the two-cycle method based on the solution of the beam-column differential equation. MethodsX, 11, 102248. doi:10.1016/j.mex.2023.102248.

[10] Ansell, A., Hallgren, M., Holmgren, J., Lagerblad, B., & Westerberg, B. (2013). Concrete Structures. Report 143, KTH Royal Institute of Technology, Stockholm, Sweden.

[11] Dundar, C., Tokgoz, S., Tanrikulu, A. K., & Baran, T. (2008). Behaviour of reinforced and concrete-encased composite columns subjected to biaxial bending and axial load. Building and Environment, 43(6), 1109–1120. doi:10.1016/j.buildenv.2007.02.010.

[12] Abd-Elhamed, M. K., & Owida, M. E. (2019). Effect of stirrups densification on ultimate capacity of rectangular reinforced concrete columns. Structures, 20, 728–764. doi:10.1016/j.istruc.2019.06.016.

[13] Dat, P. X., & Vu, N. A. (2020). An experimental study on the structural performance of reinforced concrete low-rise building columns subjected to axial loading. Journal of Science and Technology in Civil Engineering (STCE) - NUCE, 14(1), 103–111. doi:10.31814/stce.nuce2020-14(1)-09.

[14] Afefy, H. M., & El-Tony, E. T. M. (2016). Simplified Design Procedure for Reinforced Concrete Columns Based on Equivalent Column Concept. International Journal of Concrete Structures and Materials, 10(3), 393–406. doi:10.1007/s40069-016-0132-0.

[15] Bond, A. J., Brooker, O., Harris, A. J., Harrison, T., Moss, R. M., Narayanan, R. S., & Webster, R. (2006). How to design concrete structures using Eurocode 2. Concrete Centre, London, United Kingdom.

[16] Ngo, D. Q., Nguyen, H. C., Mai, D. L., & Vu, V. H. (2020). Experimental and numerical evaluation of concentrically loaded RC columns strengthening by textile reinforced concrete jacketing. Civil Engineering Journal (Iran), 6(8), 1428–1442. doi:10.28991/cej-2020-03091558.

[17] ISO 15630-1:2019. (2019). Steel for the reinforcement and prestressing of concrete - Test methods - Part 1: Reinforcing bars, rods and wire. International Organization for Standardization (ISO), Geneva, Switzerland.

[18] BS EN 12390-2:2019. (2019). Testing hardened concrete - Part 2: Making and curing specimens for strength tests. British Standards Institution (BSI), London, United Kingdom.

[19] BS EN 12390-3:2019. (2019). Testing hardened concrete - Part 3: Compressive strength of test specimens. . British Standards Institution (BSI), London, United Kingdom.

[20] Al-Abbas, B., Abdul Rasoul, Z. M. R., Hasan, D., & Rasheed, S. E. (2023). Experimental Study on Ultimate Strength of Steel Tube Column Filled with Reactive Powder Concrete. Civil Engineering Journal (Iran), 9(6), 1344–1355. doi:10.28991/CEJ-2023-09-06-04.

[21] Dinh, H. T., Ngo, D. Q., Ho, H., & Nguyen, H. C. (2023). Experimental and numerical evaluation of axial compression strengthening for corroded square reinforced concrete columns by carbon textile reinforced concrete. IOP Conference Series: Materials Science and Engineering, 1289(1), 012083. doi:10.1088/1757-899x/1289/1/012083.

[22] Xu, L., Zhou, P., Chi, Y., Huang, L., Ye, J., & Yu, M. (2018). Performance of the High-Strength Self-Stressing and Self-Compacting Concrete-Filled Steel Tube Columns Subjected to the Uniaxial Compression. International Journal of Civil Engineering, 16(9), 1069–1083. doi:10.1007/s40999-017-0257-9.

[23] O'Brien, M. (2018). Product News: AutoCAD 2019 Including Specialized Toolsets Now Available. AutoCAD 2019, Autodesk, San Francisco, United States. Available online: https://www.autodesk.com/blogs/autocad/introducing-autocad-2019-autocad-lt-2019/ (accessed on December 2023).

[24] OriginLab Corporation. (2024). OriginPro. Northampton, United States. Available online: https://www.originlab.com/ (accessed on January 2024).

[25] BS EN 206. (2013). Concrete. British Standards Institution (BSI), London, United Kingdom.

[26] European Concrete Platform. (2017). Eurocode 2 Commentary. European Concrete Platform ASBL, Brussels, Belgium. Available online: https://www.theconcreteinitiative.eu/images/ECP_Documents/Eurocode2_Commentary.pdf (accessed on January 2024).